Level Crossing Determination of $\tau(^1P_1)$ and $g_J(^3P_1)$ in Zinc and the hfs of Zn^{65} and Zn^{67}[†]

A. Landman[‡] and R. Novick[*]

Columbia Radiation Laboratory, Columbia University, New York, New York

(Received 14 November 1963)

Optical detection of level crossing in the $(4s4p)$ $^3P_1$ state of stable Zn^{67} and of 245-day Zn^{65}, using the intercombination line at 3076 Å, has resulted in a precise determination of the ratios of the dipole and quadrupole hyperfine coupling constants in each of the isotopes to the Landé g_J factor of this state. Using these results and the values of the dipole coupling constant for each isotope, as determined from double resonance experiments, we obtain the following values for the atomic g factor and "isolated" quadrupole interaction constants: Zn^{67}: $g_J = 1.501006(8)$ and $B = -18.770(12)$ Mc/sec, Zn^{65}: $g_J = 1.500984(20)$ and $B = 2.867(12)$ Mc/sec. The results for B agree with those obtained from double resonance, indicating the adequacy of our treatment of the second-order fine-structure corrections. The lifetime (τ) of the $(4s4p)$ $^1P_1$ state of Zn has been determined to be $\tau = (1.38 \pm 0.05) \times 10^{-9}$ sec through the observation of the zero-field level crossing (Hanle effect), using the resonance line at 2138 Å. These latter experiments were performed with natural zinc (96% even isotopes), and included the quantitative determination of coherence narrowing.

I. INTRODUCTION

ATOMIC fine structure, hyperfine structure, Landé g factors, and lifetimes of excited atomic states may be precisely determined by use of the optical "level-crossing" technique. The experimental simplicity and high resolution of this method make it particularly attractive. It is noteworthy that the crossing "resonances" occur at zero frequency and are therefore not subject to Doppler broadening.

Level crossings result in a change in the angular distribution of resonance fluorescence. In the case of nonreactive elements such as zinc the atoms under study are conveniently contained in an evacuated scattering bulb. The atomic vapor of the isotope of interest is illuminated with resonance radiation from a suitable lamp. The scattering system is placed in a homogeneous, variable magnetic field, which is slowly and continuously varied until a change is observed in the fluorescence scattered in a particular direction.

Quantities of interest such as the fine or hyperfine coupling constants and the Landé g factors are obtained by considering them as parameters in the appropriate Hamiltonian for the system; these constants are adjusted until the degeneracies in the theoretical energy spectrum occur at the observed crossing fields.

The level-crossing effect occurs when the excited states of interest are separated in energy by no more than their natural (or radiation) widths. Thus, the width of the level-crossing resonance provides a measure of the lifetime of the excited state τ. In the case of long-lived states $(\tau = 10^{-6}$ sec or longer), such as the $(4s4p)^3P_1$ state of zinc, the linewidths may be limited by instrumental effects such as inhomogeneities in the magnetic field or by collision effects. In the case of short-lived states $(\tau = 10^{-8}$ sec or shorter), such as the $(4s4p)^1P_1$ state of zinc $(\tau \simeq 1.4 \times 10^{-9}$ sec), the natural broadening is large compared to these effects, and τ can be accurately determined from the width of the observed crossing resonances.

The double resonance experiments of Brossel and Bitter[1] and others[2] have resulted in the determination of fine-structure splittings, hyperfine coupling constants, and lifetimes of excited atomic states. Colegrove et al.[3] discovered the phenomenon of "level crossing." They observed the crossing of two pairs of Zeeman components of the 2^3P state of helium and obtained the fine structure to high precision. Theoretical papers on the phenomenon of level crossing have been published by Breit,[4] by Franken,[5] and by Rose and Carovillano.[6] Recently, the related phenomenon of "anticrossing" was observed by Eck, Foldy, and Wieder.[7]

High precision hyperfine-structure measurements using the level crossing technique were made by Hirsch[8] and Dodd[9] on the $(6s6p)^3P_1$ state of various Hg isotopes, and by Thaddeus and Novick[10] on the $(5s5p)^3P_1$ state of Cd. The extension of this technique to the $(4s4p)^3P_1$ state of Zn is straightforward, and can be used to determine g_J and the hyperfine coupling constants of different isotopes, provided the dipole coupling constant for one isotope is known, for instance, from a double-resonance experiment.

[1] J. Brossel and F. Bitter, Phys. Rev. 86, 308 (1952).

[2] G. W. Series, Rept. Progr. Phys. 22, 280 (1959).

[3] F. D. Colegrove, P. A. Franken, R. R. Lewis, and R. H. Sands, Phys. Rev. Letters 3, 420 (1959).

[4] G. Breit, Rev. Mod. Phys. 5, 91 (1933).

[5] P. A. Franken, Phys. Rev. 121, 508 (1961).

[6] M. E. Rose and R. L. Carovillano, Phys. Rev. 122, 1185 (1961).

[7] T. G. Eck, L. L. Foldy, and H. Wieder, Phys. Rev. Letters 10, 239 (1963).

[8] H. R. Hirsch, Bull. Am. Phys. Soc. 5, 274 (1960); J. Opt. Soc. Am. 51, 1192 (1961).

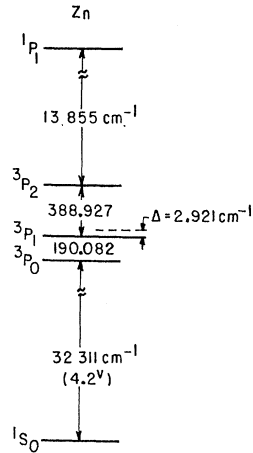[9] J. N. Dodd, Proc. Phys. Soc. (London) 77, 669 (1961); 78, 65 (1961).

[10] P. Thaddeus and R. Novick, Phys. Rev. 126, 1774 (1962).

FIG. 1. Energy level diagram for zinc.

Double-resonance measurements to obtain the lifetimes of excited states from the width of the resonances have been performed by Byron, McDermott, and Novick[11] in the $(5s5p)^3P_1$ state of Cd and by Byron et al.[12] in the $(4s4p)^3P_1$ state of Zn. The lifetimes of the corresponding singlet states, which are of the order of 10^{-9} sec, are amenable to direct measurement by observation of the zero-magnetic-field level crossing (Hanle effect). By using this method, the lifetime of the $(5s5p)^1P_1$ state of Cd was measured by Lurio and Novick.[13] This was extended to the $(4s4p)^1P_1$ state of Zn in the work presented here. In both the latter sets of experiments, coherence narrowing was observed.

The pertinent energy-level diagram for the experiments on zinc is shown in Fig. 1.

II. THEORY

For transitions from a single ground state $|a\rangle$ to two excited states $|b\rangle$ and $|c\rangle$, which are well separated in energy, Franken[5] obtains for the rate $R(\mathbf{f},\mathbf{g})$, in arbitrary units, at which photons of incoming polarization $\mathbf{f}$ and outgoing polarization $\mathbf{g}$ are scattered:

$$R(\mathbf{f},\mathbf{g})=R_0=|f_{ab}|^2|g_{ba}|^2+|f_{ac}|^2|g_{ca}|^2, \qquad (1)$$

where $f_{ab}=\langle a|\mathbf{f}\cdot\mathbf{r}|b\rangle$, etc.

In the vicinity of crossing, $R=R_0+S$, as given below:

$$R(\mathbf{f},\mathbf{g})=R_0+\frac{A+A^*}{1+4\pi^2\tau^2\nu^2(b,c)}+\frac{(A-A^*)2\pi i\tau\nu(b,c)}{1+4\pi^2\tau^2\nu^2(b,c)}, \qquad (2)$$

where $A=f_{ba}f_{ac}g_{ab}g_{ca}$, τ is the mean lifetime of the two excited states, and $\nu(b,c)=(E_b-E_c)/h$.

The apparatus was arranged so that the photodetector would receive light scattered through 90° by the atomic vapor (see Fig. 2). In the hfs studies of Zn^{65} and Zn^{67} the magnetic field was perpendicular to

[11] F. Byron, M. N. McDermott, and R. Novick, Phys. Rev. (to be published).
[12] F. Byron, M. N. McDermott, R. Novick, B. Perry, and E. Saloman, Phys. Rev. **134**, A47 (1964).
[13] A. Lurio and R. Novick, Phys. Rev. (to be published).

the plane formed by the incoming and outgoing light beams and no polarizers were employed. In the $^1P_1$ lifetime work the static magnetic field was oriented parallel to the path of the incoming light, and the incident light was polarized with its electric vector parallel to the detector light path (Fig. 5). In both of these cases the signal resulting from the crossing of two levels with m values differing by two ($\Delta m=2$ crossings) produced a crossing resonance with a Lorentz shape.[6]

The width of the crossing resonance is determined by the lifetime of the atomic states and their rate of approach. If ΔH is the full width at half-intensity of the resonance in field units then we find

$$\Delta H=\frac{1}{\pi\tau\partial\nu(b,c)/\partial H}, \qquad (3)$$

where τ is the lifetime and $\partial\nu(b,c)/\partial H$ is the rate at which the levels approach each other in frequency units. In the case of the zero-field level crossings (Hanle effect) we have

$$\frac{\partial\nu(b,c)}{\partial H}=\frac{2g_J\mu_0}{h} \quad \text{and} \quad \Delta H=\frac{\hbar}{\tau g_J\mu_0}, \qquad (4)$$

where g_J is the Landé g factor and $\hbar$ and μ_0 have their usual meaning. The factor 2 arises because we observe $\Delta m=2$ transitions. In the case of high-field crossings $\partial\nu/\partial H$ must be evaluated from the appropriate energy-level diagram. In order to improve the signal-to-noise ratio, narrow-band lock-in techniques were employed with small-amplitude Zeeman modulation. Lorentz resonances are effectively differentiated and the observed signal has a dispersion shape. The separation of the peaks of the dispersion curve (δH) is related to the Lorentz half-width (ΔH) by

$$\Delta H=\sqrt{3}(\delta H). \qquad (5)$$

This result is, of course, only valid if the modulation amplitude is small compared to δH.

The hyperfine-structure parameters can be obtained from a knowledge of the "crossing" fields. In order to do this we must first diagonalize the Zeeman and hfs Hamiltonian for a range of values of the parameters. We select those parameters which most nearly reproduce the observed crossings. The Hamiltonian for zinc includes the sum of direct hyperfine and Zeeman terms, plus second-order corrections due to other fine-structure states. We use the Hamiltonian given by Lurio, Mandel, and Novick,[14]

$$\mathfrak{IC}=\sum_i [\mathbf{T}_e^{(1)}(i)\cdot\mathbf{T}_n^{(1)}+\mathbf{T}_e^{(2)}(i)\cdot\mathbf{T}_n^{(2)}]$$
$$+\mu_0 g_s\mathbf{S}\cdot\mathbf{H}+\mu_0 g_L\mathbf{L}\cdot\mathbf{H}+\mu_0 g_I\mathbf{I}\cdot\mathbf{H}, \qquad (6)$$

in which the tensors $\mathbf{T}_e$ and $\mathbf{T}_n$ refer to hyperfine operators in the electron and nuclear subspaces, re-

[14] A. Lurio, M. Mandel, and R. Novick, Phys. Rev. **126**, 1758 (1962).

TABLE I. Expected relative signal/background for the four crossings for Zn^{67} and Zn^{65}.

Crossing	Expected relative signal/background (arbitrary units)
Main	1.0
First foldover	0.11
Second foldover	0.07
Third foldover	0.02

spectively, with (1) referring to dipole operators and (2) to quadrupole operators. The sum over i refers to the two valence electrons in the sp configuration of the $^3P_1$ state of zinc. The matrix elements between the $^3P_1$ and $^3P_2$ and $^3P_0$ states, are included only to second order by the method of Van Vleck. There are four $\Delta m = 2$ crossings for a $^3P_1$ state atom with $I = \frac{5}{2}$. In the absence of quadrupole and second-order effects these four crossings would coalesce at the field $H_c = 3A/g_J'\mu_0$, where g_J is the Landé g factor. In the above expression, H_c is the crossing field, and A is the hyperfine dipole coupling constant for the $^3P_1$ states. The quadrupole coupling and the second-order effects lift the crossing degeneracy and we find that the spacing of the crossings provides a sensitive measure of B.

The signal-to-background ratio for the main level crossing is of the order of 1%. If this ratio is arbitrarily assigned the value unity, we obtain the following estimates for the expected signal-to-background ratios for the four crossings (see Table I).

III. EXPERIMENTAL

Triplet State Experiments

A schematic diagram of the apparatus used for the observation of the $^3P_1$ state of Zn^{67} and Zn^{65} is shown in Fig. 2. An electrodeless rf discharge lamp was used to produce light (of the order of 10^{18} photons/sec of the 3076 Å intercombination line) which was transmitted through a set of two 4-in.-diam quartz condensing lenses and impinged on the scattering cell. Two types of scattering cells were used, one spherical
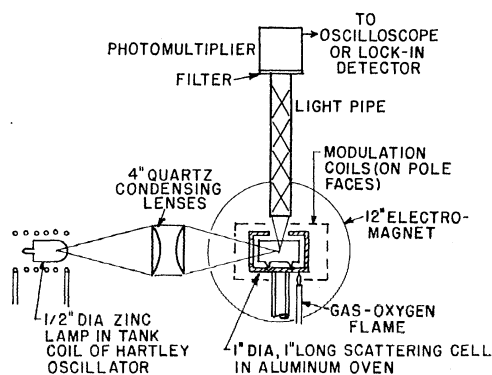
FIG. 2. Schematic diagram of the apparatus used for observation of level crossings in the $^3P_1$ state of Zn^{67} and Zn^{65}.

and the other cylindrical (with typical dimensions of 1 in.). These scattering cells were contained in an aluminum oven which was heated by a gas-oxygen flame. Flame heat was used in preference to electrical heating in order to avoid any possible stray magnetic fields. All materials used in the construction of the oven were carefully tested for magnetic contamination. The scattering cell was placed at the center of a 12-in. Harvey-Wells electromagnet (Model L-128) having a homogeneity of about 1 part in 10^5 over the cell region. The magnetic field was applied perpendicular to the direction of the incoming and scattered light, which was collected by a light pipe oriented at right angles to the incoming light. At the end of the light pipe, Schott UG-11 filter passed the light at 3076 Å (but excluded the true resonance line at 2138 Å) into a photomultiplier tube and associated circuits; from there the signal went to a phase-sensitive, lock-in detector, and finally to a recorder. The steady field at which crossing occurred was modulated by a small magnetic field at 30 cps, and the observed signal was the derivative of the level-crossing resonance curve under the conditions of the experiment. The theoretical
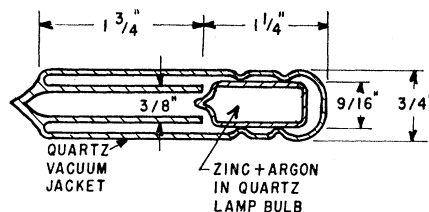
FIG. 3. Zinc lamp bulb and vacuum jacket.

line shape is Lorentzian (cf. section on "Theory"), and we expect a dispersion-type derivative curve.

The lamp used originally contained a small sphere of quartz about $\frac{1}{2}$-in. in diameter, which was baked out at 1000°C for about a day under high vacuum, then purged with an intense argon discharge, loaded with a small amount of predistilled zinc and argon at a pressure of about 2 Torr, and then sealed off. This bulb was placed in the tank coil of a Hartley oscillator operating at a few Mc/sec and exciting a discharge within the bulb. The lifetime of such a bulb was limited to several hours by the chemical reaction between the quartz and Zn. This reaction severely limited the output of the lamp and sometimes produced gross instabilities in the discharge. A cylindrical bulb proved slightly better. A great improvement was obtained by encasing the cylindrical bulb in a quartz vacuum jacket to maintian the necessary high temperature for the Zn discharge with low rf excitation (cf. Fig. 2). This procedure substantially prolonged the useful lifetime of the lamp.

The scattering cells or bulbs were also baked at high temperatures and purged with a high-frequency vacuum discharge produced by a Tesla coil located adjacent to the bulb. No argon discharge was used in the case of

the cells since the net effect of it was to produce "gassy" cells. After the discharge cleaning, the bulbs were filled with the appropriate Zn isotope. The bulbs were attached to the vacuum system with small quartz tabulations. After the filling process, the bulbs were sealed off, and these tubulations formed small extensions to the bulb. In use the tubulations were maintained at a lower temperature than the rest of the cell and thus determined the vapor pressure of the zinc. A non-magnetic copper-constantan thermocouple was placed in a hole near the top of the oven containing the cells, and contiguous to the tubulations. The thermocouple readings served as a useful index of the cell temperature; typically the oven was heated until the thermocouple reading was about 380°C.

The crossing fields were determined to an accuracy of about 1 part in 10^5 with a proton NMR magnetometer containing a mineral oil sample. The proton resonance frequency was determined with a Hewlett-Packard model 524D electronic counter. Unfortunately, it was necessary to locate the proton sample about an

FIG. 4. Sample hyperfine level crossing curve for Zn⁶⁷; the numbers indicate the magnetic field in terms of the proton resonance frequency in kilocycles.
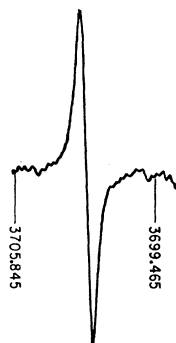
inch or more from the Zn oven and to correct for the small field difference that existed between the proton probe and the zinc sample. The difference field was determined by replacing the Zn sample with a second NMR magnetometer, and measuring the difference frequency for the two magnetometers. The difference field was determined before and after each set of crossing observations; the typical corrections were about 30 ppm. The actual dispersion-type curves were traced on chart paper, a sample curve being shown in Fig. 4. Markers on the chart recorded proton resonance frequencies on both sides of the traced curves. Averages of resonance curves for both increasing and decreasing magnetic field were combined to form an over-all average for each level crossing. Further discussion is deferred to the section on "Results."

Lifetime of the ¹P₁ State

A schematic diagram of the experimental arrangement used for the determination of the lifetime of the ¹P₁ state of zinc is shown in Fig. 5. The measurements necessitated varying H over a range of 100 G on either
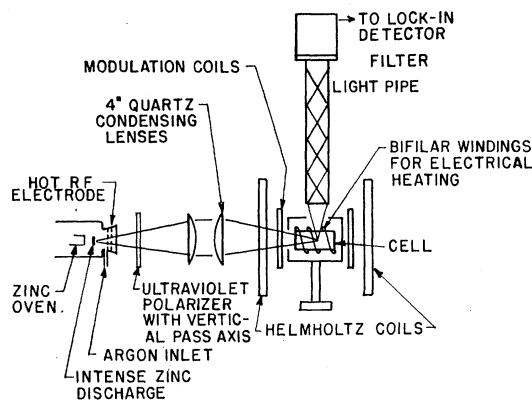
FIG. 5. Schematic diagram of the apparatus used for the determination of the lifetime of the ¹P₁ state of zinc.

side of zero magnetic field, and a simple electromagnet consisting of a set of Helmholtz coils was used. The lamp for producing the resonance radiation was a flow lamp (capable of producing 10^{15} photons/sec or more of the 2138-Å resonance line) shown in Fig. 6. This lamp, of the Cario-Lochte-Holtgreven type, was developed by Lurio and Novick, and a complete description of it will be published elsewhere.[15]

For the singlet state experiments, the light from the lamp was transmitted through a set of two 4-in. quartz lenses and impinged on a scattering cell of the cylindrical type which had been filled with naturally occurring zinc (96% even isotopes). The small amount of Zn⁶⁷ present (4%) had a negligible effect on the results. The scattering cell was placed inside an electrically heated oven, wound with bifilar heater windings to minimize the magnetic fields due to the heating current. (Since the ¹P₁ state resonances are from 50 to 100 G wide, the small residual fields arising from the electrical heater were not important.) The oven was placed on a stand at the center of the Helmholtz coils. Modulation was provided by an additional set of coils situated inside the main Helmholtz pair. The modulation field was parallel to the main field. Since the magnetic field was
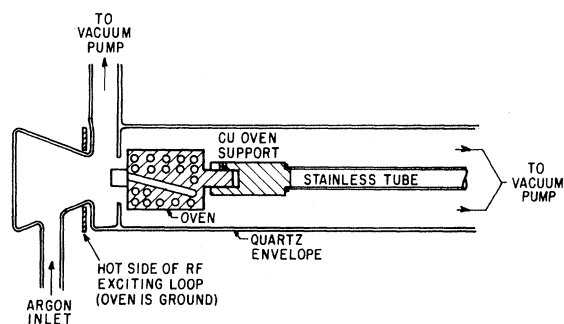
FIG. 6. Flow discharge lamp.

¹⁵ H. Bucka, B. Budick, A. Lurio, and R. Novick (to be published).

applied parallel to the incoming light, a polarizer with a pass axis along the direction of detection (perpendicular to the incoming light) was necessary, as was discussed in the section on "Theory." The scattered light was collected into a light pipe. The rest of the experimental apparatus was essentially identical with that used for the triplet state measurements, except that an interference filter passing the 2138-Å resonance line was used rather than the UG-11 filter.

The scattering cells were identical to those used in the high-field level-crossing experiments and require no further discussion. The temperature was determined with a thermocouple, but in this set of experiments, more carefully, since it was essential to know the temperature to determine the density of zinc atoms in the study of coherence narrowing. However, the value for the lifetime τ at low densities, is practically independent of temperature, and does not require a precise knowledge of the temperature.

The magnetic field was determined by measuring the current through the Helmholtz coils. The magnetic field was calibrated with a NMR magnetometer. The current was measured using a Leeds and Northrup potentiometer, on which the voltage across a fixed resistance could be read directly. As the magnetic field was varied through resonance, markers were made on the chart paper at periodic intervals, corresponding to the voltage readings in millivolts. A typical dispersion-type resonance curve is shown in Fig. 7, giving the peak-to-peak separation of the curve in millivolts, and the cell temperature at which the measurements were made.

IV. RESULTS AND DISCUSSION

Lifetime of the $(4s4p)^1P_1$ State of Zinc

The lifetime measurements were described in the previous setion. A typical Hanle effect curve is shown in Fig. 7. The peak-to-peak separation of the derivative curve obtained on the chart was measured in millivolts on the potentiometer, and this value translated into the corresponding value for the magnetic field in G. This result for the dispersion-type curve was multiplied by $\sqrt{3}$ to obtain the Lorentzian half width (ΔH). A correction for modulation broadening of the line must
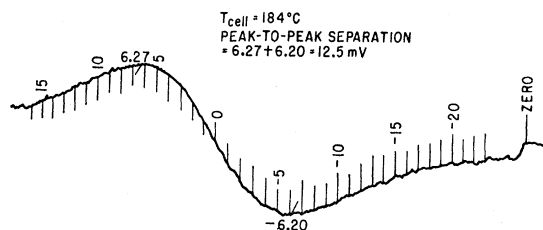

FIG. 7. Hanle effect signal for the $^1P_1$ state as obtained with Zeeman modulation and lock-in detection. The marks and numbers indicate the magnetic field in terms of current shunt readings.

then be included. Lurio[16] has shown that

$$\Delta H_{\text{corrected}} = \frac{\Delta H}{1+3[\tau\pi(\partial\nu/\partial H)h]^2},\qquad(7)$$

where h is the peak-to-peak field modulation and the other symbols have been defined above.

Typically the correction was between one and two percent. In Sec. II we showed that the lifetime of the state (τ) is related to the full width at half-maximum (ΔH) of the zero-field level-crossing curve by

$$\tau = \frac{\hbar}{g_J\mu_0\Delta H}.\qquad(8)$$

Taking $g_J(^1P_1)=1.00$ we find

$$\tau = 113.5\times10^{-9}/\Delta H \text{ (sec)}\qquad(9)$$

when ΔH is expressed in G.

TABLE II. Zinc singlet-state data and results, including coherence narrowing.

Cell temperature (°C)	Vapor density (atoms/cc)	$\Delta H_{\text{corrected}}$ Width of curve (Gauss)	Coherence time (nsec)
139	8.7×10^8	81.8	1.39
140	9.6×10^8	81.6	1.39
145	1.48×10^9	80.2	1.41
154	3.2×10^9	78.2	1.45
161	5.6×10^9	74.7	1.52
166	8.8×10^9	73.1	1.55
177	1.91×10^{10}	68.6	1.65
184	3.2×10^{10}	64.5	1.76
197	8.0×10^{10}	52.3	2.17
200	9.8×10^{10}	49.0	2.32
218[a]	3.2×10^{11}	(36)	(3.2)

[a] These results were obtained with very poor signal-to-noise ratios and are not as reliable as the other data.

The apparent lifetime depends on the vapor pressure of zinc in the cell because of the effect of multiple scattering or trapping of the resonance fluorescence. Barrat[17] has developed the theory of this effect, including the effects of size and shape of cells.

In order to relate the measured temperature in the cell to the vapor pressure of the zinc and the density of zinc atoms, we used the results of Dushman,[18]

$$\ln P = A - (B/T),\qquad(10)$$

with P in microns, $A=11.94$, $B=6.744\times10^3$. We used the ideal gas formula to obtain the density, n, from P and T:

$$n = \frac{9.66\times10^{-5}}{T}P \text{ (in microns)};\qquad(11)$$

[16] A. Lurio (private communication).
[17] J. P. Barrat, J. Phys. Radium 20, 541, 633, 657 (1959).
[18] S. Dushman, Scientific Foundations of Vacuum Technique (John Wiley & Sons, Inc., New York, 1949).

where n is density in atoms/cc and T is in degrees Kelvin.

The results are given in Table II, where we have listed cell temperature, zinc vapor density, width of curve in Gauss, and coherence time. A graph of coherence time versus vapor density is given in Fig. 8. The shape of the curve is in agreement with the predictions of Barrat's theory.[17] By extrapolating to zero density, we obtain the lifetime of the $(4s4p)^1P_1$ state of zinc: $(1.38\pm0.05)\times10^{-9}$ sec. This value is substantially lower than previous results, which ranged from 1.7 to 2.3×10^{-9} sec. One possible explanation for these high values is that the observations were made under high density conditions where coherence narrowing was significant.

Hyperfine Structure and g Factor for the $(4s4p)^3P_1$ State of Zn^{65} and Zn^{67}

High-field level crossings can be used to determine the dipole and quadrupole coupling constants of the
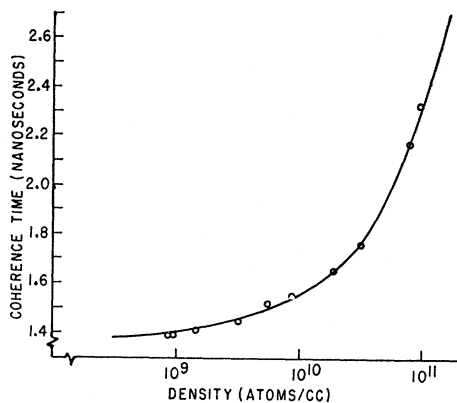
FIG. 8. Density dependence of the coherence time for the $^1P_1$ state of zinc.

isotopes of one element, as well as the Landé g_J factor, provided one value among these is known from another source.

A diagram of the energy levels in a magnetic field for the $^3P_1$ state with $I=\frac{5}{2}$ will serve to clarify the discussion. Fig. 9 shows the levels of interest for positive nuclear dipole moment and negative nuclear quadrupole moment. This case holds for Zn^{65}. Zn^{67}, which has a positive nuclear quadrupole moment, has the foldover crossings[19] on the opposite side of the main crossing from those for Zn^{65}. However, the ordering remains the same. The main "level crossing" is the one involving the $(F=\frac{7}{2}, m=-\frac{7}{2})$ and $('F'=\frac{5}{2}, m=-\frac{3}{2})$ states. The first fold-over crossing and the one nearest in magnetic field to the main crossing is that of the $('F'=\frac{5}{2}, m=\frac{1}{2})$ and $('F'=\frac{5}{2}, m=-\frac{3}{2})$ states. In order, the next two are

---

[19] Foldover crossings are defined as crossings of two levels, both of which are generated from the same value of F at zero magnetic field.

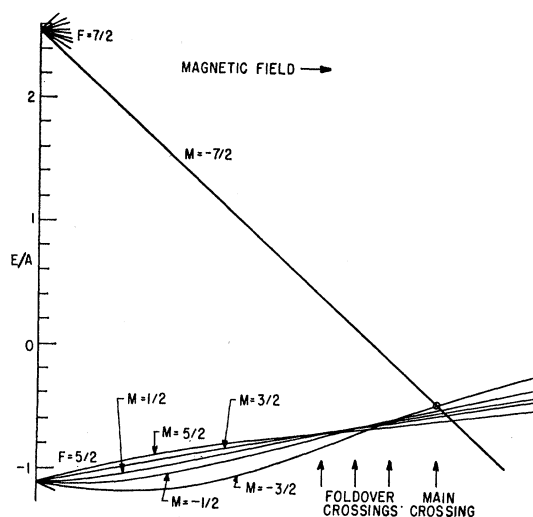FIG. 9. Zeeman energy levels of interest for level crossings in the $^3P_1$ state of Zn^{65}; in the case of Zn^{67} the foldover crossings occur on the high-field side of the main crossing.

always the $('F'=\frac{5}{2}, m=\frac{3}{2})$ and $('F'=\frac{5}{2}, m=-\frac{1}{2})$, and the $('F'=\frac{5}{2}, m=\frac{5}{2})$ and $('F'=\frac{5}{2}, m=\frac{1}{2})$ crossings. Arrows in Fig. 9 indicate the positions of these crossings for the general case. The main crossing is very sensitive to the ratio of A to g_J (as will be shown later), and the spacing between crossings is sensitive to the value of B.

In the case of Zn^{67}, all four crossings for which the two degenerate levels differ in m_F by two were observed. The magnetic-field values at which crossings were observed to occur, measured in units of the nuclear magnetic resonance frequency of protons in mineral oil, together with the low-field assignment of the levels are: $('F',m_F)=(\frac{7}{2}, -\frac{7}{2})$ and $(\frac{5}{2}, -\frac{3}{2})$ at 3702.755 ± 0.020 kc/sec; $(\frac{5}{2},\frac{1}{2})$ and $(\frac{5}{2}, -\frac{3}{2})$ at 3807.79 ± 0.20 kc/sec; $(\frac{5}{2},\frac{3}{2})$ and $(\frac{5}{2}, -\frac{1}{2})$ at 3922.95 ± 0.30 kc/sec; and $(\frac{5}{2},\frac{5}{2})$ and $(\frac{5}{2},\frac{1}{2})$ at 4094.4 ± 0.6 kc/sec. The crossings were progressively weaker and broader in the order listed above. The signal-to-noise ratios decreased from more than 100 to 1 to about 2 to 1. At least sixteen different determinations were made for each of the crossing fields. The quoted uncertainty is two times the standard deviation.

In the case of Zn^{65}, three $\Delta m=2$ crossings were observed. The crossing fields, in units of the nuclear magnetic resonance frequency of protons in mineral oil, together with the low field assignment of the levels, are: $('F',m_F)=(\frac{7}{2}, -\frac{7}{2})$ and $(\frac{5}{2}, -\frac{3}{2})$ at 3253.52 ± 0.06 kc/sec; $(\frac{5}{2}, \frac{1}{2})$ and $(\frac{5}{2}, -\frac{3}{2})$ at 3238.0 ± 0.3 kc/sec; $(\frac{5}{2}, \frac{3}{2})$ and $(\frac{5}{2}, -\frac{1}{2})$ at 3221.9 ± 0.4 kc/sec.

Data on the second and third crossings were obtained from four and six curves, respectively, with signal-to-noise ratios never better than 2 to 1. The major crossing was determined from fourteen curves obtained on two separate dates (eight on one, six on the other), with signal-to-noise ratios of about 10 to 1.

Interpretation of the above results requires an ex-

planation of the diagonalization procedure for the Hamiltonian, including effects due to the nearby fine structure states, and an explanation of the procedure for obtaining A, B, and g_J from the data.

The Hamiltonian is given again below:

$$\mathcal{H}' = \sum_i \sum_k \mathbf{T}_e^{(k)}(i) \cdot \mathbf{T}_n^{(k)} + \mu_0 g_s \mathbf{S} \cdot \mathbf{H}$$

$$+ \mu_0 g_L \mathbf{L} \cdot \mathbf{H} + \mu_0 g_I \mathbf{I} \cdot \mathbf{H}, \quad (6)$$

the terms being defined previously. In addition to the elements diagonal in J, we must also consider the off-diagonal matrix elements which connect the $^3P_1$ state to the nearby $^3P_2$ and $^3P_0$ states. We include these to second order by the method of Van Vleck, and the corrected matrix is diagonalized. The second-order corrections are of the order of 10^{-4} times the direct matrix elements. Typical matrix elements to be inserted are given in the paper of Lurio, Mandel, and Novick.[14] The 3×3 matrix which must finally be diagonalized (for arbitrary I) is given in Appendix I. It should be noted that only the ratios A/g_J' and B/g_J' can be obtained, since we necessarily lose one piece of information when we determine only the zeros of the spectrum rather than finite frequencies.

An explicit analytic expression for the main level crossing, relating the crossing field to the hyperfine coupling constants and atomic and nuclear moments, can be obtained. It is given here for the cases of Zn^{67} and Zn^{65} ($I = \frac{5}{2}$). This expression was obtained by substituting the eigenvalue for the $F = \frac{7}{2}$, $m = -\frac{7}{2}$ state into the secular equation for the $m = -\frac{3}{2}$ states. This procedure yields a quadratic equation for H_c which can be readily solved by noting that the terms containing δ_0 and δ_2 are of the order of 10^{-4}. (There is a trivial and uninteresting solution at $H = 0$.) The expression which is then obtained for the crossing is

$$\frac{3A'(1+3b/10)(1-3b/40)}{g_J'\mu_0 H_c}$$

$$= 1 + 9b/40 + \frac{1}{2}\frac{1-3b/20+81b^2/1600}{1+9b/40}G$$

$$+ \frac{1}{27}\frac{(1+9b/40)(1+9b/40)}{(1+3b/10)(1-3b/40)}\frac{(\alpha\mu_0 H_c)^2}{A'}$$

$$\times [1/\delta_0 - 1/(8\delta_2)] + \frac{1}{3\sqrt{6}}\frac{(1+9b/40)}{(1+3b/10)}\frac{\alpha\mu_0 H_c}{A'}\frac{A_0}{\delta_0}$$

$$- \frac{1}{6\sqrt{3}}\frac{(1-3b/40+27b^2/800)}{(1+3b/10)(1-3b/40)}\frac{\alpha\mu_0 H_c}{A'}\frac{A_2}{\delta_2}$$

$$+ \frac{1}{5\sqrt{3}}\frac{(1+27b/80+81b^2/1280)}{(1+3b/10)(1-3b/40)}\frac{\alpha\mu_0 H_c}{A'}\frac{B_2}{\delta_2}, \quad (12)$$

where H_c is the crossing field, and δ_0 and δ_2 are the

absolute values of the $^3P_0 - ^3P_1$ and $^3P_2 - ^3P_1$ intervals. A' and B' are the dipole and quadrupole coupling constants as they would be determined in a zero-field double resonance experiment without second-order corrections, and $b = B'/A'$. A and B are the interaction constants obtained after applying the second-order corrections, i.e., these are the coupling constants that would obtain if the $^3P_{2,1,0}$ fine-structure splitting was very large. g_J' is the Landé factor that would be determined in a low-field Zeeman experiment on the spin-zero zinc isotopes.[20] $G = g_I/g_J'$, with g_I negative for a positive nuclear moment and g_J' positive. The remaining constants are given by

$$A = [(c_2^2/2 - c_1^2/4)a_s + \frac{1}{2}c_2^2 a_{1/2}$$
$$+ ((5/4)c_1^2 - (5/16)\sqrt{2}\xi c_1 c_2)a_{3/2}],$$

$$B = [c_1^2/2 - \sqrt{2}\eta c_1 c_2]b_{3/2},$$

$$A_0 = c_2(a_s - a_{1/2}) - (c_1 5\xi/4\sqrt{2})a_{3/2},$$

$$A_2 = c_1 a_s - [c_1 + c_2(5\xi/4\sqrt{2})]a_{3/2},$$

$$B_2 = (c_1 + c_2\eta\sqrt{2})b_{3/2}.$$

Here a_s, $a_{1/2}$, and $a_{3/2}$ are the dipole coupling constants for the s electron, and the p electron in the $j = \frac{1}{2}$ and $j = \frac{3}{2}$ states, respectively; these are evaluated in Appendix II. The quadrupole coupling constant for the p electron in the $j = \frac{3}{2}$ state is $b_{3/2}$. ξ and η are relativistic factors as defined by Schwartz.[21] c_1 and c_2 are constants determined by the coupling between the electrons (in this case, almost pure Russell-Saunders coupling). These can be evaluated from the ratio of the lifetimes of the triplet and singlet states.

An inspection of Eq. (12) shows that the leading contribution of B' is smaller than that of A' by the ratio $(B'/A')^2$. Thus, the main level crossing can give a good first approximation to the ratio A'/g_J' (provided B'/A' is small, ~ 0.1 or less).

The other three crossings do not permit a simple analytic solution, although a computer program without second-order corrections was used to give approximate values for A', B', and g_J'. In order to obtain the final corrected values for A, B, and g_J', a trial-and-error procedure was employed with the help of a computer program for diagonalization. We used trial values for A, B, and g_J'; these, together with the second-order corrections computed from them, and the experimental values for the crossing fields were inserted into the matrix elements shown in Appendix I. A diagonalization was then made on the computer, and the eigenvalues of the crossing states compared. The set of trial values resulting in the smallest sum for the squares of differences of the eigenvalues for each pair of crossing levels was taken as the final set. With the final set of parameters the mean energy difference between the nominally degenerate levels was two kilocycles per second.

[20] In the case of odd isotopes the apparent g factor is modified by second order hyperfine-Zeeman terms.
[21] C. Schwartz, Phys. Rev. 97, 380 (1955); 105, 173 (1957).

Analysis of the Van Vleck transformed matrix has led to the conclusion that only the ratios A/g_J' and B/g_J' can be determined independently. Since the same situation holds for Zn⁶⁵, four of the five quantities of interest can be determined from our experiments on level crossing. Using the values of A for Zn⁶⁷ and Zn⁶⁵, as determined from zero-field double resonance experiments by Byron et al.[12] $[A(67)=609.086(2)$ Mc/sec and $A(65)=535.163(2)$ Mc/sec], the following results are obtained for g_J', for the corrected values for B both for Zn⁶⁷ and Zn⁶⁵, and for the average value for g_J' for the $^3P_1$ state of zinc:

$$Zn^{67}: \quad g_J' = 1.501006(8),$$
$$B = -18.770(12) \text{ Mc/sec};$$
$$Zn^{65}: \quad g_J' = 1.500984(20),$$
$$B = 2.867(12) \text{ Mc/sec};$$
$$g_J'(^3P_1) \quad = 1.501000(12).$$

The corresponding values for B obtained from the double resonance experiments[12] are:

$$Zn^{67}: \quad B = -18.783(8) \text{ Mc/sec};$$
$$Zn^{65}: \quad B = 2.870(5) \text{ Mc/sec}.$$

One significant result of the analysis described here is the excellent agreement between the results of level-crossing and double resonance experiments, provided the second-order corrections are included. If we neglect the second-order corrections, the values for $B(67)$ which are obtained become

$$\text{Double resonance}: B' = -19.331(7);$$
$$\text{Level crossing}: \quad B' = -19.757(10).$$

It is clear that the second-order corrections are essential and that we have an adequate theory for the hyperfine and Zeeman interactions in the $^3P_1$ state, including the effects due to the $^3P_0$ and $^3P_2$ states. It is also evident that possible configuration-mixing effects are negligible.

In reducing the data we used the result of Liebes and Franken[22] for the proton magnetic moment in Bohr magnetons.

The ratio $Q(65)/Q(67)$ can be determined from the values given above for B, and we obtain $Q(65)/Q(67)$ $= -0.1527(8)$.

A theoretical estimate of g_J is given by the expression

$$g_J = \tfrac{1}{2}\alpha^2(g_l+g_s)+\beta^2 g_l+\Delta, \qquad (13)$$

where $g_s=2(1.0011596)$ and $g_l=1-Km/M(\text{Zn})$. The quantity Δ is included to indicate that there are unevaluated diamagnetic, relativistic, and possible nuclear structure corrections.[23] The coefficient K is of the order

of unity.[24] Below we show that $\alpha^2=0.999792$ and $\beta^2=2.08\times10^{-4}$. Using these values we find

$$g_J=1.501039(15),$$

where the uncertainty is based solely on the uncertainties in α and β and the estimated range of possible K values. We have not included any estimate of the possible effects of configuration interaction.

The constants α^2 and β^2 were determined from the lifetimes of the triplet and singlet states, rather than from the $(4s4p)$ fine-structure intervals, since the theory of the fine structure is not completely in hand. The relation between the lifetimes and coefficients is

$$\frac{\alpha^2}{\beta^2}=\frac{\tau(^3P_1)\cdot\lambda^3(^1P_1-{}^1S_0)}{\tau(^1P_1)\cdot\lambda^3(^3P_1-{}^1S_0)}. \qquad (14)$$

The lifetime of the triplet state is $(2.0\pm0.2)\times10^{-5}$ sec, as determined by F. Byron et al.[12] and the lifetime of the singlet state is given above. The constants α and β are related to c_1 and c_2 used earlier by

$$\alpha=(\tfrac{1}{3})^{1/2}c_1+(\tfrac{2}{3})^{1/2}c_2,$$
$$\beta=(\tfrac{2}{3})^{1/2}c_1-(\tfrac{1}{3})^{1/2}c_2. \qquad (15)$$

The experimentally determined value for g_J', 1.501000(12), can be compared to the theoretical value of 1.501039(15) obtained from Eq. (13). The difference is $-39(27)\times10^{-6}$. The major contribution to this difference comes from relativistic and diamagnetic corrections (cf. Abragam and Van Vleck[25] and, to a lesser degree, from nuclear structure effects.[23] A meaningful calculation of these requires Hartree-Fock, or better, wave functions for the valence electrons in zinc. These have not yet been obtained. However, this difference of 39 parts in 10⁶ appears very reasonable in view of results obtained by Lurio in neon and argon,[26] by Abragam and Van Vleck in oxygen,[25] and by Thaddeus and Novick in cadmium.[10] In addition, a calculation of the relativistic correction alone in the case of the $(6s6p)^3P_1$ state of mercury, using Hartree-Fock wave functions,[27] gave a value of -50×10^{-6}.

ACKNOWLEDGMENTS

[22] S. Liebes and P. Franken, Phys. Rev. **116**, 633 (1959).

[23] V. W. Hughes, article in *Recent Research in Molecular Beams*, edited by I. Estermann (Academic Press Inc., New York, 1959).

[24] M. F. Crawford, W. M. Gray, F. M. Kelly, and A. L. Schawlow, Can. J. Res. **A28**, 138 (1950).

[25] A. Abragam and J. H. Van Vleck, Phys. Rev. **92**, 1448 (1953).

[26] A. Lurio, G. Weinreich, C. W. Drake, V. W. Hughes, and J. A. White, Phys. Rev. **120**, 153 (1960).

[27] B. Mishra, Proc. Cambridge Phil. Soc. **48**, 511 (1952).

APPENDIX I

Hfs and Zeeman Matrix Elements for a $(sp)^3P_1$ State with Arbitrary Nuclear Spin I, Including the Second Order Contributions from the $^3P_0$ and $^3P_2$ States

$$H'_{I+1,I+1}=\left[\frac{1}{I+1}g_{J}'+\frac{I}{I+1}g_{I}\right]M\mu_0H+IA+\tfrac{1}{4}B-\frac{\{\alpha(g_s-g_l)\mu_0H\}^2}{\delta_2}\left\{\frac{(7I+4)(I+1)-M^2}{12(I+1)(2I+1)}\right\}$$

$$+\frac{\{\alpha(g_s-g_l)\mu_0H\}^2}{\delta_0}\left\{\frac{2}{3(I+1)(2I+1)}[(I+1)^2-M^2]\right\}-\frac{\alpha(g_s-g_l)\mu_0H}{\delta_2}\left\{\frac{MI}{I+1}\sqrt{3}\left[\frac{A_2}{4}-\frac{B_2}{8I}\right]\right\}$$

$$-\frac{3I(I+2)}{16}\frac{[A_2-(1/2I)B_2]^2}{\delta_2}.$$

$$H'_{I,I}=\left[\frac{1}{I(I+1)}g_{J}'+\frac{I^2+I-1}{I(I+1)}g_{I}\right]M\mu_0H-A-\frac{2I+3}{4I}B-\frac{\{\alpha(g_s-g_l)\mu_0H\}^2}{\delta_2}\left\{\frac{1}{4}+\frac{M^2}{12I(I+1)}\right\}$$

$$+\frac{\{\alpha(g_s-g_l)\mu_0H\}^2}{\delta_0}\left\{\frac{2M^2}{3I(I+1)}\right\}-\frac{\alpha(g_s-g_l)\mu_0H}{\delta_2}\left\{\frac{M(2I+3)}{I(I+1)}\sqrt{3}\left[\frac{2I-1}{12}A_2+\frac{1}{8I}B_2\right]\right\}$$

$$+\frac{\alpha(g_s-g_l)\mu_0H}{\delta_0}M(\tfrac{2}{3})^{1/2}A_0-\frac{(2I+3)(2I-1)}{16}\frac{\{A_2+[3/2I(2I-1)]B_2\}^2}{\delta_2}+\tfrac{1}{4}I(I+1)\frac{A_0^2}{\delta_0}.$$

$$H'_{I-1,I-1}=\left[-\frac{1}{I}g_{J}'+\frac{I+1}{I}g_{I}\right]M\mu_0H-(I+1)A+\frac{(I+1)(2I+3)}{4I(2I-1)}B-\frac{\{\alpha(g_s-g_l)\mu_0H\}^2}{\delta_2}\left[\frac{(7I+3)I-M^2}{12I(2I+1)}\right]$$

$$+\frac{\{\alpha(g_s-g_l)\mu_0H\}^2}{\delta_0}\left\{\frac{2}{3I(2I+1)}[I^2-M^2]\right\}-\frac{\alpha(g_s-g_l)\mu_0H}{\delta_2}\left\{\frac{M(I+1)}{I}\sqrt{3}\left[\frac{A_2}{4}+\frac{2I+3}{8I(2I-1)}B_2\right]\right\}$$

$$-\frac{3(I+1)(I-1)}{16}\frac{\{A_2+[2I+3/2I(2I-1)]B_2\}^2}{\delta_2}.$$

$$H'_{I+1,I}=-\frac{(g_{J}'-g_{I})\mu_0H}{I+1}\left(\frac{I}{(2I+1)}[(I+1)^2-M^2]\right)^{1/2}-\frac{\{\alpha(g_s-g_l)\mu_0H\}^2}{\delta_2}\left\{\frac{M}{12I(I+1)}\right.$$

$$\times\left.\left(\frac{I}{(2I+1)}[(I+1)^2-M^2]\right)^{1/2}\right\}+\frac{\{\alpha(g_s-g_l)\mu_0H\}^2}{\delta_0}\left\{\frac{2M}{3I(I+1)}\left(\frac{I}{(2I+1)}[(I+1)^2-M^2]\right)^{1/2}\right\}$$

$$-\frac{\alpha(g_s-g_l)\mu_0H}{\delta_2}\left\{\frac{1}{2(I+1)}\left(\frac{3I}{(2I+1)}[(I+1)^2-M^2]\right)^{1/2}\right\}\left\{\frac{I+7}{12}A_2-\frac{I+3}{8I}B_2\right\}$$

$$+\frac{\alpha(g_s-g_l)\mu_0H}{\delta_0}\left(\frac{I}{(2I+1)}\frac{[(I+1)^2-M^2]}{6}\right)^{1/2}A_0.$$

$$H'_{I,I-1}=-\frac{(g_{J}'-g_{I})\mu_0H}{I}\left(\frac{I+1}{2I+1}[I^2-M^2]\right)^{1/2}+\frac{\{\alpha(g_s-g_l)\mu_0H\}^2}{\delta_2}\left\{\frac{M}{12I(I+1)}\left(\frac{I+1}{2I+1}[I^2-M^2]\right)^{1/2}\right\}$$

$$-\frac{\{\alpha(g_s-g_l)\mu_0H\}^2}{\delta_0}\left\{\frac{2M}{3I(I+1)}\left(\frac{I+1}{2I+1}[I^2-M^2]\right)^{1/2}\right\}+\frac{\alpha(g_s-g_l)\mu_0H}{\delta_2}\left\{\frac{1}{2I}\left(\frac{I+1}{2I+1}\frac{[I^2-M^2]}{3}\right)^{1/2}\right\}$$

$$\times\left\{\frac{I-6}{4}A_2+\frac{3(I-2)(2I+3)}{8I(2I-1)}B_2\right\}-\frac{\alpha(g_s-g_l)\mu_0H}{\delta_0}\left(\frac{I+1}{2I+1}\frac{[I^2-M^2]}{6}\right)^{1/2}A_0.$$

$$H'_{I+1,I-1}=\frac{\{\alpha(g_s-g_l)\mu_0H\}^2}{\delta_2}\left\{\frac{1}{12(2I+1)}\left(\frac{[I^2-M^2][(I+1)^2-M^2]}{I(I+1)}\right)^{1/2}\right\}$$

$$-\frac{\{\alpha(g_s-g_l)\mu_0H\}^2}{\delta_0}\left\{\frac{2}{3(2I+1)}\left(\frac{[I^2-M^2][(I+1)^2-M^2]}{I(I+1)}\right)^{1/2}\right\}.$$

Note: In the matrix elements, A and B are the "isolated" hyperfine coupling constants (including second-order corrections); all the symbols are defined in the main body of the text.

APPENDIX II

Calculation of Individual-Electron hfs Coupling Constants

The dipole and quadrupole interaction constants for the $^3P_2$ and $^3P_1$ states may be written in terms of the individual electron interaction constants as follows:

$$A(^3P_2)=\tfrac{1}{4}a_s+\tfrac{3}{4}a_{3/2},$$

$$A(^3P_1)=\tfrac{1}{4}(2c_2{}^2-c_1{}^2)a_s+[(5/4)c_1{}^2-(5\sqrt{2}/16)c_1c_2\xi]a_{3/2}$$
$$+\tfrac{1}{2}c_2{}^2a_{1/2},$$

$$B(^3P_2)=b_{3/2},$$

$$B(^3P_1)=\tfrac{1}{2}(c_1{}^2-2\sqrt{2}\eta c_1c_2)b_{3/2}.$$

The expressions $A(^3P_1)$ and $B(^3P_1)$ were given previously as A and B. The expression for $B(^3P_2)$ need not be used for the determination of a_s, $a_{1/2}$, $a_{3/2}$, and $b_{3/2}$, but one further relationship between the a's is required. We will use

$$a_{1/2}=5\theta(1-\delta)(1-\epsilon)a_{3/2},$$

as given in Lurio.[28]

Table III lists the constants used for obtaining the individual electron interaction constants and for evaluating the second-order hfs corrections. c_1 and c_2 are obtained from the lifetimes of the $^3P_1$ and $^1P_1$ states. The other constants are taken directly from the paper of Lurio.[28]

TABLE III. Constants used for obtaining the individual electron interaction constants and for evaluating the second-order hfs corrections.

Constant	Value of constant
c_1	0.5654
c_2	0.8247
ξ	1.01
η	1.03
θ	1.095
$(1-\delta)(1-\epsilon)$	0.981

[28] A. Lurio, Phys. Rev. 126, 1768 (1962).

In Table IV are given the values for the pertinent total dipole and quadrupole interaction constants, including the second order corrections. $A(^3P_1)$ for both Zn⁶⁷ and Zn⁶⁵ are taken from Byron et al.[12] $B(^3P_1)$ for both Zn⁶⁷ and Zn⁶⁵ are obtained by averaging the results from the work of Byron, et al.[12] and from that presented here. $A(^3P_2)$ for Zn⁶⁷ is taken directly from Lurio.[28] $A(^3P_2)$ for Zn⁶⁵ is obtained by considering the

TABLE IV. Values of the hfs interaction constants, including the second-order corrections.

hfs interaction constant	Zn⁶⁷(Mc/sec)	Zn⁶⁵(Mc/sec)
$A(^3P_1)$	609.086	535.163
$B(^3P_1)$	−18.776	2.868
$A(^3P_2)$	531.996	467.429

ratio for A in the $^3P_2$ state of the two isotopes to be equal to the ratio for A in the $^3P_1$ state.

The results for the values for the interaction constants in the $^3P_1$ state differ slightly from those of Lurio[28] for the following reasons: (a) The uncorrected values for A and B have now been determined more precisely; (b) A small mathematical error in evaluating the second-order corrections by Lurio gave incorrect results

TABLE V. Values of the individual electron hyperfine interaction constants, including the second-order corrections.

Individual electron interaction constant	Zn⁶⁷(Mc/sec)	Zn⁶⁵(Mc/sec)
a_s	1992.4	1750.5
$a_{1/2}$	242.7	213.2
$a_{3/2}$	45.2	39.7
$b_{3/2}$	36.1	−5.5

in his paper (however, his conclusions, especially pertaining to the value of the quadrupole moment, remain valid).

Finally, in Table V, we list the values for the individual electron hyperfine interaction constants, including the second-order corrections. One iteration has proven sufficient in determining these within the experimental error.